

# Scheme to Achieve Silicon Topological Photonics

Long-Hua Wu\* and Xiao Hu†

<sup>1</sup>*International Center for Materials Nanoarchitectonics (WPI-MANA),  
National Institute for Materials Science, Tsukuba 305-0044, Japan*

<sup>2</sup>*Graduate School of Pure and Applied Sciences, University of Tsukuba, Tsukuba 305-8571, Japan*  
(Dated: March 3, 2015)

We derive in the present work topological photonic states purely based on silicon, a conventional dielectric material, by deforming a honeycomb lattice of silicon cylinders into a triangular lattice of cylinder hexagons. The photonic topology is associated with a pseudo time reversal (TR) symmetry constituted by the TR symmetry respected in general by the Maxwell equations and the  $C_6$  crystal symmetry upon design, which renders the Kramers doubling in the present photonic system with the role of pseudo spin played by the circular polarization of magnetic field in the transverse magnetic mode. We solve Maxwell equations, and demonstrate new photonic topology by revealing pseudo spin-resolved Berry curvatures of photonic bands and helical edge states characterized by Poynting vectors.

PACS numbers: 03.65.Vf, 42.70.Qs, 73.43.-f

**Introduction.**—The discovery of quantum Hall effect (QHE) opened a new chapter of condensed matter physics with topology as the central concept [1–11]. Topological states are not only interesting in an academic point of view, but also expected to yield significant impacts to applications because robust surface (or edge) states protected by bulk topology provide new possibilities for spintronics and quantum computation [12–17]. However, topological matters confirmed so far are still limited in number, and most of them exhibit topological properties only at very low temperatures, which hinders their better understanding and manipulation indispensable for practical applications.

Photonic crystals are optical analogues of solids with lattice of atoms replaced by medium of periodic electric permittivity and/or magnetic permeability [18]. Meta-materials are designed to generate electromagnetic (EM) properties such as negative index, magnetic lens, and so on, which are not available in nature [19]. Recently it has been recognized that topological states characterized by unique edge propagations of EM wave can be realized in photonic crystals based on gyromagnetic materials under external magnetic field, bi-anisotropic meta-materials with coupled electric and magnetic fields where bi-anisotropy acts as effective spin-orbit coupling, and coupled resonator optical waveguides (CROWs) [20–31]. (for a review see [32]).

In the present work, we propose a two-dimensional (2D) photonic crystal purely made of silicon, a conventional dielectric material. We notice that a honeycomb lattice is equivalent to a triangular lattice of hexagonal clusters composed by six neighboring sites, and that, taking this larger hexagonal unit cell instead of the primitive rhombic unit cell of two sites (see Fig. 1(a)), the Dirac cones at K and K' points in the first Brillouin zone of honeycomb lattice are folded to doubly degenerate Dirac cones at  $\Gamma$  point. It is then intriguing to observe that at the  $\Gamma$  point there are two 2D irreducible representa-

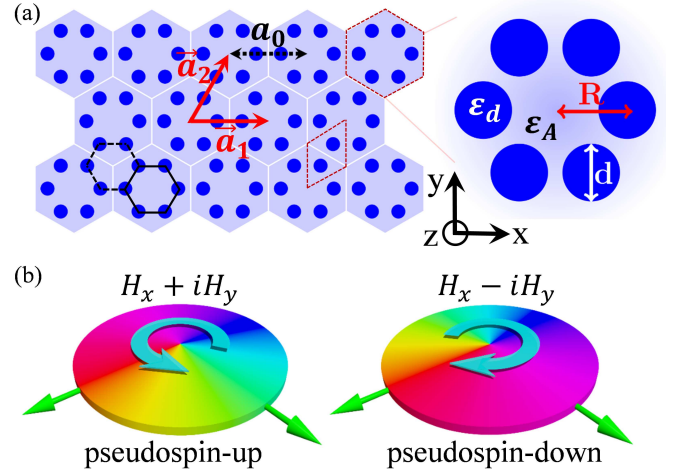


FIG. 1. (a) Schematics of a triangular photonic crystal of "artificial atoms" composed by six cylinders of dielectric material with dielectric constant  $\epsilon_d$  along the  $z$  direction embedded in the environment of dielectric constant  $\epsilon_A$ . Red dashed rhombus and hexagon are primitive cells of honeycomb and triangular lattices respectively. Solid black hexagon labels an artificial atom, while dashed black one marks interstitial regions among atoms.  $\vec{a}_1$  and  $\vec{a}_2$  are lattice vectors, and  $a_0$  is the lattice constant of triangular lattice. Right panel: enlarged view of hexagonal cluster with  $R$  the length of hexagon edge and  $d$  the diameter of cylinders. (b) Pseudo spin states of the present photonic system associated with the left- and right-hand circular polarizations of magnetic fields  $H_x \pm iH_y$  of the TM mode.

tions in  $C_6$  symmetry group associated with odd and even parity respective to spatial inversion operation. Based on these properties, we propose to open a topologically non-trivial band gap by deforming the honeycomb lattice in the way keeping hexagonal clusters and preserving the  $C_6$  rotation symmetry (see Fig. 1(a)). Explicitly, we reveal by solving the Maxwell equations that harmonic EM modes hosted by the hexagonal cluster, working as "ar-

tificial atom” in the present scheme, exhibit electronic orbital-like  $s$ -,  $p$ -, and  $d$ -wave shapes and form photonic bands. We clarify that there is a pseudo time reversal (TR) symmetry constituted by the TR symmetry respected by the Maxwell equations and the  $C_6$  crystal symmetry upon design, which behaves in the same way as TR symmetry in electronic systems and renders the Kramers doubling in the present photonic system. This intimately gives the one-to-one correspondence between the left- and right-hand circular polarizations of magnetic field in the transverse magnetic (TM) mode and the up- and down-spin states of electrons. Evaluating the Berry curvatures of photonic bands and the edge states for finite systems, we demonstrate the emergence of topological phases. With the simple design free of requirement on any external field and gyromagnetic or bi-anisotropic materials, the present topological photonic states purely based on silicon are expected very promising for future applications.

*Artificial atom and pseudo spin.*—Let us consider harmonic TM modes of EM wave, namely those of finite in-plane  $H_x$ ,  $H_y$ , out-of-plane  $E_z$  components and with others being zero, in a dielectric medium (for coordinates see Fig. 1(a)). For simplicity, the real electric permittivity is taken frequency independent in the regime under consideration. The master equation for a harmonic mode of frequency  $\omega$  is then derived from the Maxwell equations [33]

$$\left[ \frac{1}{\varepsilon(\mathbf{r})} \nabla \times \nabla \times \right] E_z(\mathbf{r}) = \frac{\omega^2}{c^2} E_z(\mathbf{r}), \quad (1)$$

with  $\varepsilon(\mathbf{r})$  the position-dependent permittivity and  $c$  the speed of light. The transverse components of magnetic field are given by the Faraday relation  $\mathbf{H} = -i/(\mu_0\omega)\nabla \times \mathbf{E}$ , where the magnetic permeability  $\mu_0$  is presumed as that of vacuum. The Bloch theorem applies for the present system when  $\varepsilon(\mathbf{r})$  is periodic in space as shown schematically in Fig. 1(a). It is reminded however that the master equation (1) describes the EM waves instead of electrons carrying on the spin degree of freedom, with the most prominent difference lying at the response upon TR operation.

Our photonic crystal is made of cylinders of dielectric material with relative permittivity  $\varepsilon_d$  (such as silicon) parallel to the  $z$  axis embedded in a dielectric background of  $\varepsilon_A$  (such as air) as schematically shown in Fig. 1(a). Six dielectric cylinders of diameter  $d$  form a hexagon with edge length  $R$ . Our discussions below are for states uniform along the  $z$  axis, which reduces the problem to 2D. We start from a honeycomb lattice of dielectric cylinders, and deform it in the way keeping hexagonal clusters composed by six neighboring cylinders and the  $C_6$  symmetry. Now the alignment of dielectric cylinders is more convenient to be considered a triangular lattice of hexagonal “artificial atoms”. There are two 2D irreducible representations in the  $C_6$  symmetry group associated with the

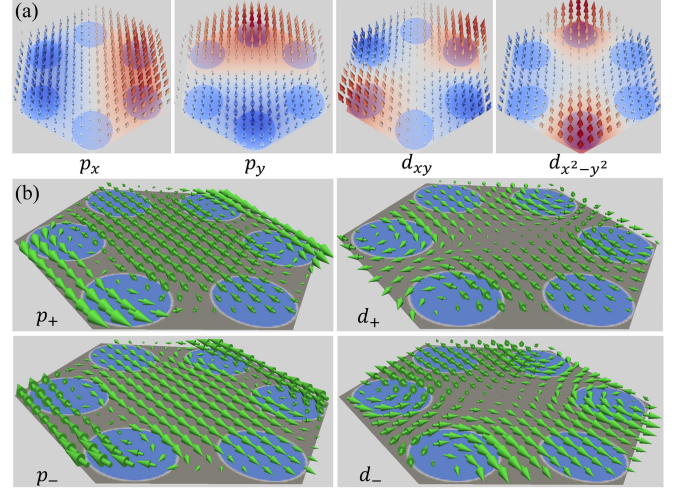


FIG. 2. (a) Electric field  $E_z$  of the  $p_x/p_y$  and  $d_{xy}/d_{x^2-y^2}$  photonic orbitals hosted by the artificial atom. (b) Two pseudo spin states corresponding to the left- and right-hand circular polarizations of magnetic fields  $H_x \pm iH_y$  associated with  $E_z$  fields of positive and negative angular momenta:  $p_{\pm}$  and  $d_{\pm}$ .

triangular lattice:  $E'$  and  $E''$  with basis functions  $x/y$  and  $xy/(x^2 - y^2)$ , corresponding to odd and even spatial parities respectively [34]. As can be seen from  $E_z$  fields in Fig. 2(a) obtained by solving Eq. (1), the artificial atoms carry  $p_x/p_y$  and  $d_{xy}/d_{x^2-y^2}$  orbitals, with the same symmetry as those of electronic orbitals of conventional atoms in solids.

We now examine matrix representations of  $\pi/3$  rotation and its combinations for the basis functions of  $p_x/p_y$  and  $d_{xy}/d_{x^2-y^2}$ . Since  $p_x/p_y$  behave in the same way as  $x/y$ , it is easy to see

$$D_{E'}(C_6) \begin{pmatrix} p_x \\ p_y \end{pmatrix} = \begin{pmatrix} \frac{1}{2} & -\frac{\sqrt{3}}{2} \\ \frac{\sqrt{3}}{2} & \frac{1}{2} \end{pmatrix} \begin{pmatrix} p_x \\ p_y \end{pmatrix}. \quad (2)$$

It is noticed that  $\mathcal{U} = [D_{E'}(C_6) + D_{E'}(C_6^2)]/\sqrt{3} = -i\sigma_y$  with  $D_{E'}(C_6^2) \equiv D_{E'}^2(C_6)$  is associated with the  $\pi/2$  rotation of  $p_x/p_y$  ( $\sigma_y$  being the Pauli matrix). Therefore,  $\mathcal{U}^2(p_x, p_y)^T = -(p_x, p_y)^T$ , which is consistent with the odd parity of  $p_x/p_y$  with respect to spatial inversion. Similarly, one has

$$D_{E''}(C_6) \begin{pmatrix} d_{x^2-y^2} \\ d_{xy} \end{pmatrix} = \begin{pmatrix} -\frac{1}{2} & -\frac{\sqrt{3}}{2} \\ \frac{\sqrt{3}}{2} & -\frac{1}{2} \end{pmatrix} \begin{pmatrix} d_{x^2-y^2} \\ d_{xy} \end{pmatrix}, \quad (3)$$

which, in the matrix form, is same as  $D_{E'}(C_6^2)$  because the basis functions are now bilinear of  $x/y$ . It is then straightforward to check that  $[D_{E''}(C_6) - D_{E''}(C_6^2)]/\sqrt{3} = \mathcal{U}$  is associated with a  $\pi/4$  rotation of  $d_{xy}/d_{x^2-y^2}$ , which yields  $\mathcal{U}^2(d_{x^2-y^2}, d_{xy})^T = -(d_{x^2-y^2}, d_{xy})^T$ .

We compose the antiunitary operator  $\mathcal{T} = \mathcal{U}\mathcal{K}$  where  $\mathcal{K}$  is the complex conjugate operator associated with the

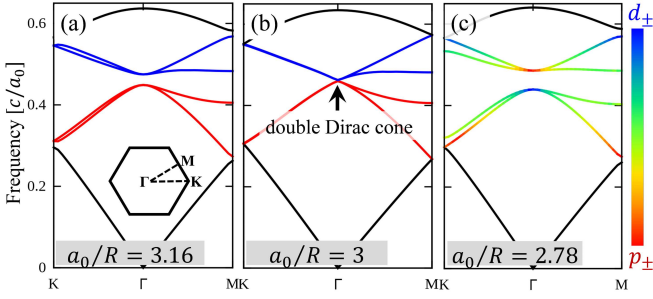


FIG. 3. Dispersion relations of TM mode for the 2D photonic crystals with  $\varepsilon_d = 11.7$ ,  $\varepsilon_A = 1$  and  $d = 2R/3$  for (a)  $a_0/R = 3.16$  (Inset: Brillouin zone of triangular lattice), (b)  $a_0/R = 3$  and (c)  $a_0/R = 2.78$ . Blue and red are for  $d_{\pm}$  and  $p_{\pm}$  bands respectively, and rainbow for hybridization between them. The case of  $a_0/R = 3$  corresponds exactly to the honeycomb lattice of individual cylinders. Diameter of individual cylinders is kept the same for all calculations since its variation influences photonic bands slightly in quantitative manners.

TR operation respected by Maxwell systems in general. Since  $\mathcal{T}^2 = -1$  is guaranteed by  $\mathcal{U}^2 = -1$ ,  $\mathcal{T}$  can be taken as a pseudo TR operator which provides Kramers doubling in the same way of electronic systems. It is clear that the crystal symmetry plays an important role in this pseudo TR symmetry [35].

The two pseudo spin states are given by

$$p_{\pm} = (p_x \pm ip_y)/\sqrt{2}; \quad d_{\pm} = (d_{x^2-y^2} \pm id_{xy})/\sqrt{2}, \quad (4)$$

which are related to the above basis functions by unitary transformation. Namely the pseudo spin up and down correspond to the wave functions of  $E_z$  fields of positive and negative angular momenta, or equivalently the left- and right-hand circular polarizations of in-plane magnetic fields defined by  $H_x \pm iH_y$  as shown in Figs. 1(b) and 2(b).

Pseudo spins discussed so far in photonic systems include bonding/antibonding states of electric and magnetic fields [24, 25], left-hand/right-hand circular polarizations of EM waves [28], and clockwise/anticlockwise circulations of light in CROWs [29, 30]. The first two implementations involve sophisticated metamaterial structures and thus require delicate fabrications. While the last one only uses silicon fibers, and thus easy to prepare, a break in one of coupling loops at perimeter induces a "magnetic impurity" which destroys the topological helical edge states.

*Photonic bands.*—Now we calculate the photonic band dispersions described by the master equation (1) imposing periodic boundary conditions along unit vectors  $\vec{a}_1$  and  $\vec{a}_2$  given in Fig. 1(a). As shown in Fig. 3, double degeneracy in the band dispersions appears at  $\Gamma$  point, which can be identified as  $p_{\pm}$  and  $d_{\pm}$  states, consistent with the symmetry consideration. For large lattice constant  $a_0$ , the photonic band below (above) the gap is oc-

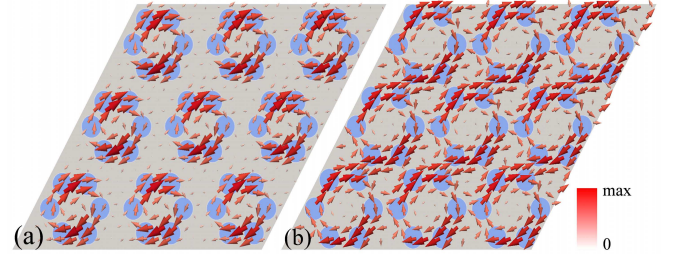


FIG. 4. Real-space distributions of the time-averaged Poynting vector associated with the pseudo spin-down state at  $\Gamma$  point below the photonic gap: (a)  $a_0/R = 3.16$  in the trivial regime and (b)  $a_0/R = 2.78$  in the topological regime.

cupied by  $p_{\pm}$  ( $d_{\pm}$ ) states (see Fig. 3(a) for  $a_0/R = 3.16$ ).

Reducing the lattice constant to  $a_0/R = 3$ , the  $p$  and  $d$  states become degenerate at  $\Gamma$  point, and two Dirac cones appear as shown in Fig. 3(b). This is because that at this lattice constant the system is equivalent to honeycomb lattice of individual cylinders, and the doubly degenerate Dirac cones are nothing but those at K and K' point in the Brillouin zone of honeycomb lattice based on the primitive rhombic unit cell of two sites [31].

When the lattice constant is further reduced, a global photonic band gap is reopened as shown in Fig. 3(c) for  $a_0/R = 2.78$ . Now the  $E_z$  field at low-(high-)frequency side of the band gap exhibits  $d_{\pm}$  ( $p_{\pm}$ ) characters around the  $\Gamma$  point, opposite to the order away from the  $\Gamma$  point. Namely a band inversion takes place upon reducing the lattice constant in the present photonic lattice. Quantitatively, the band gap is  $\Delta\omega = 13.8$  THz at  $\omega = 138.75$  THz with  $a_0 = 1 \mu\text{m}$ , with all the quantities scaling with the lattice constant.

In order to see what happens in the system around the band inversion, we check the real-space distribution of Poynting vector  $\vec{S} = \text{Re}[\vec{E} \times \vec{H}^*]/2$  averaged over a period  $\tau = 2\pi/\omega$ , which describes the energy flow in the present EM system. It is found that the Poynting vector is circling around individual atoms as shown in Fig. 4(a) for  $a_0/R = 3.16$ , with the chirality of Poynting vector corresponding to the pseudo spin (Poynting vector with pseudo spin-up is not shown explicitly). The EM energy flows around individual atoms, characterizing a conventional "insulating" state. At  $a_0/R = 2.78$ , namely after the band inversion, the Poynting vectors are much enhanced in interstitial regimes as shown in Fig. 4(b). It is in a sharp contrast to the case in Fig. 4(a), and implies an unconventional insulating state.

*Topological edge state.*—We also consider a ribbon of photonic crystal after band inversion by cladding its two edges in terms of two photonic crystals with trivial band gap (namely before band inversion) at the same frequency window, which prevents possible edge states from leaking into free space. It should be kept in mind that, since the cluster of six cylinders is the basic block of the



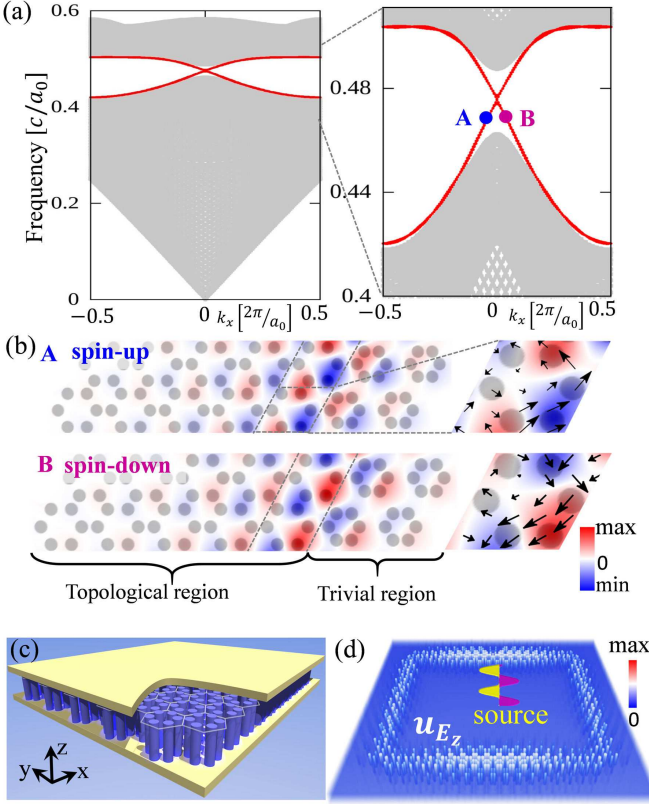


FIG. 5. (a) Dispersion relation of a ribbon-shaped topological photonic crystal, which is infinite in one direction and of 45 and 6 artificial atoms for the topological and trivial regions respectively in the other direction. Right panel: enlarged view of (a). Red curves are for topological edge states.  $A$  and  $B$  are two points where  $E_z$  field are shown in (b). Parameters used here are same as those in Fig. 3 except  $a_0/R = 2.9$  and  $a_0/R = 3.125$  in topological and trivial regions respectively. (b) Real-space distributions of  $E_z$  fields at points  $A$  and  $B$ . Right panels: time-averaged Poynting vectors  $\vec{S}$  over a period. (c) Photonic crystal of height  $h$  with two horizontal gold plates placed at two ends symmetrically. Hexagons in fade white color are primitive cells for the triangular lattice. (d) Distribution of energy-density carried by  $E_z$  field  $u_{E_z}(\mathbf{r}) = \epsilon(\mathbf{r})|E_z(\mathbf{r})|^2/2$  in a topological photonic crystal cladded by a trivial one with  $h = 10$  mm,  $d = 2.4$  mm and  $a_0 = 10$  mm, and  $R = 3.65$  mm and 3 mm in topological and trivial regions respectively. Frequency of harmonic line source is  $\omega = 13.47$  GHz within the photonic band gap.

present design, it should not be destroyed for any meaningful discussion. As displayed in Fig. 5(a), there appears edge states as indicated by the double degenerated red curves, with a small gap (not noticeable in this scale) opened at  $\Gamma$  point due to the suppression of  $C_6$  symmetry and then pseudo TR symmetry at the interface. Checking real-space distribution of  $E_z$  field at typical momenta around  $\Gamma$  point ( $A$  and  $B$  in the enlarged vision of Fig. 5(a) with  $k_x = \pm 0.04 \frac{2\pi}{a_0}$ ), we find that the in-gap states locate at the edge and decay exponentially into bulk as displayed in Fig. 5(b) (two other states are local-

ized at the other ribbon edge and not shown explicitly). As shown in the right insets of Fig. 5(b), the Poynting vectors exhibit a nonzero downward/upward EM energy flow for the pseudo spin-down/-up state even averaged over time. This indicates unambiguously counter propagations of EM energy at the sample edge associated with the two pseudo spin states, the hallmark of a quantum spin Hall effect (QSHE) state [2, 3]. Distributions of Poynting vectors of the bulk bands in Fig. 5(b) for the ribbon system are similar to those in Fig. 4(b) for the infinite system. QHE has been described by the cyclic motions of electrons under strong external magnetic field in a quasi classic picture of electronic wave functions [36]. It is noticed that the Poynting vector is a physical quantity in EM systems, and therefore the distributions shown in Figs. 4 and 5(b) can be observed in experiments. The photonic QSHE in the present system can also be confirmed by evaluating the  $\mathbb{Z}_2$  topology index based on a  $k \cdot p$  model around  $\Gamma$  point. Although Dirac dispersions in photonic systems were discussed previously in both square and triangular lattices [37–39], possible nontrivial topology was not addressed.

For experimental implementation of the present topological state, the finite height of silicon rods along  $z$  direction has to be taken into account. We consider explicitly a square sample of topological photonic crystal sandwiched by two horizontal gold plates separated by  $h$  (see Fig. 5(c)), with the height  $h$  chosen to prevent photonic bands with nonzero  $k_z$  from falling into the topological band gap. The size of topological sample is  $40\vec{a}_1 \times 20(\vec{a}_1 + \vec{a}_2)$  with all four edges cladded by a trivial photonic crystal. A harmonic line source  $\mathbf{E} = E_0 e^{i\omega t} \hat{z}$  is placed parallel to silicon rods to inject EM wave at the interface with the frequency in the topological band gap. We simulate the system by solving time-dependent Maxwell equations [41, 42]. Since any harmonic source preserves TR symmetry respected by Maxwell equations, the system exhibits helical topological edge states as shown in Fig. 5(d).

In conclusion, we derive a two-dimensional photonic crystal with nontrivial topology purely based on silicon, a conventional dielectric material, simply by deforming honeycomb lattice of silicon cylinders. A pseudo time reversal symmetry is constructed in terms of the time reversal symmetry respected by the Maxwell equation in general and the  $C_6$  crystal symmetry upon design, which enables the Kramers doubling with the role of pseudo spin played by the polarization of magnetic field of transverse magnetic mode. The present topological photonic crystal with simple design backed up by the symmetry consideration can be fabricated relatively easy as compared with other proposals, and is expected to leave impacts to the topological physics and related materials science.

The authors acknowledge K. Sakoda for useful discussions on photonic Dirac behaviors. This work was supported by the WPI Initiative on Materials Nanoarchitec-

tonics, Ministry of Education, Culture, Sports, Science and Technology of Japan, and partially by Grant-in-Aid for Scientific Research under the Innovative Area "Topological Quantum Phenomena" (No.25103723), Ministry of Education, Culture, Sports, Science and Technology of Japan.

---

\* WU.Longhua@nims.go.jp

† HU.Xiao@nims.go.jp

- [1] K. v. Klitzing, G. Dorda, and M. Pepper, Phys. Rev. Lett. **45**, 494 (1980).
- [2] M. Z. Hasan and C. L. Kane, Rev. Mod. Phys. **82**, 3045 (2010).
- [3] X.-L. Qi and S.-C. Zhang, Rev. Mod. Phys. **83**, 1057 (2011).
- [4] D. J. Thouless, M. Kohmoto, M. P. Nightingale, and M. d. Nijs, Phys. Rev. Lett. **49**, 405 (1982).
- [5] D. Xiao, M.-C. Chang, and Q. Niu, Rev. Mod. Phys. **82**, 1959 (2010).
- [6] F. D. M. Haldane, Phys. Rev. Lett. **61**, 2015 (1988).
- [7] C. L. Kane and E. J. Mele, Phys. Rev. Lett. **95**, 226801 (2005).
- [8] B. A. Bernevig, T. L. Hughes, and S.-C. Zhang, Science **314**, 1757 (2006).
- [9] D. Hsieh, D. Qian, L. Wray, Y. Xia, Y. S. Hor, R. J. Cava, and M. Z. Hasan, Nature **452**, 970 (2008).
- [10] R. Yu, W. Zhang, H.-J. Zhang, S.-C. Zhang, X. Dai, and Z. Fang, Science **329**, 61 (2010).
- [11] C.-Z. Chang *et al.*, Science **340**, 167 (2013).
- [12] D. Pesin and A. H. MacDonald, Nature Mater. **11**, 409 (2012).
- [13] Q.-F. Liang, L.-H. Wu, and X. Hu, New J. Phys. **15**, 063031 (2013).
- [14] C. Nayak, S. H. Simon, A. Stern, M. Freedman, and S. Das Sarma, Rev. Mod. Phys. **80**, 1083 (2008).
- [15] T. D. Stanescu and S. Tewari, J. Phys.: Condens. Matter **25**, 233201 (2013).
- [16] C. W. J. Beenakker, Annu. Rev. Condens. Matter Phys. **4**, 113 (2013).
- [17] L.-H. Wu, Q.-F. Liang, and X. Hu, Sci. Technol. Adv. Mater. **15**, 064402 (2014).
- [18] E. Yablonovitch, Phys. Rev. Lett. **58**, 2059 (1987).
- [19] J. B. Pendry, A. J. Holden, D. J. Robbins, and W. J. Stewart, IEEE Trans. Microw. Theory Tech. **47**, 2075 (1999).
- [20] F. D. M. Haldane and S. Raghu, Phys. Rev. Lett. **100**, 013904 (2008).
- [21] Z. Wang, Y. D. Chong, J. D. Joannopoulos, and M. Soljačić, Phys. Rev. Lett. **100**, 013905 (2008).
- [22] Z. Wang, Y. Chong, J. D. Joannopoulos, and M. Soljačić, Nature **461**, 772 (2009).
- [23] K. Fang, Z. Yu, and S. Fan, Nature Photon. **6**, 782 (2012).
- [24] A. B. Khanikaev, S. H. Mousavi, W.-K. Tse, M. Kargarian, A. H. MacDonald, and G. Shvets, Nature Mater. **12**, 233 (2013).
- [25] T. Ma, A. B. Khanikaev, S. H. Mousavi, and G. Shvets, arXiv:1401.1276 (2014).
- [26] G. Q. Liang, and Y. D. Chong, Phys. Rev. Lett. **110**, 203904 (2013).
- [27] M. C. Rechtsman *et al.*, Nature **496**, 196 (2013).
- [28] C. He, X.-C. Sun, X.-P. Liu, M.-H. Lu, Y. Chen, L. Feng, and Y.-F. Chen, arXiv:1405.2869 (2014).
- [29] M. Hafezi, E. A. Demler, M. D. Lukin, and J. M. Taylor, Nature Phys. **7**, 907 (2011).
- [30] M. Hafezi, S. Mittal, J. Fan, A. Migdall, and J. M. Taylor, Nature Photon. **7**, 1001 (2013).
- [31] T. Ochiai, Phys. Rev. B **86**, 075152 (2012); *ibid* Int. J. Mod. Phys. B. **28**, 1441004 (2013).
- [32] L. Lu, J. D. Joannopoulos, and M. Soljačić, Nature Photon. **8**, 821 (2014).
- [33] J. D. Joannopoulos, S. G. Johnson, J. N. Winn, and R. D. Meade, *Photonic Crystals: Molding the Flow of Light* (Princeton University Press, New Jersey, 2008).
- [34] M. S. Dresselhaus, G. Dresselhaus, and A. Jorio, *Group theory: Application to the physics of condensed matter* (Springer-Verlag, Berlin, Heidelberg, 2008).
- [35] L. Fu, Phys. Rev. Lett. **106**, 106802 (2011).
- [36] S. M. Girvin, *The Quantum Hall Effect: Novel Excitations and Broken Symmetries* (Springer-Verlag, Berlin, Heidelberg, 1999).
- [37] X. Huang, Y. Lai, Z. H. Hang, H. Zheng, and C. T. Chan, Nature Mater. **10**, 582 (2011).
- [38] K. Sakoda, Opt. Express **20**, 9925 (2012).
- [39] K. Sakoda, Opt. Express **20**, 3898 (2012).
- [40] S. G. Johnson, and J. D. Joannopoulos, Opt. Express **8**, 173 (2001).
- [41] A. Taflov, and S. C. Hagness, *Computational Electrodynamics: The Finite-Difference Time-Domain Method* (Artech: Norwood, MA, 2000).
- [42] A. F. Oskooi, D. Roundy, M. Ibanescu, P. Bermel, J. D. Joannopoulos, and S. G. Johnson, Comput. Phys. Commun. **181**, 687 (2010).